A photometric study of an EW-type binary system: GV Leo

Wichean Kriwattanawong[1,2] and Panomporn Poojon[1]

[1] Department of Physics and Materials Science, Faculty of Science, Chiang Mai University,
    Chiangmai 50200, Thailand; *k.wichean@gmail.com*
[2] National Astronomical Research Institute of Thailand, Chiangmai 50200, Thailand

Abstract A photometric study of a contact binary system, GV Leo is presented. New observations were done using the *BVR* filter bands. We find that a revised orbital period is 0.26673171 d and the orbital period of this system is decreasing at a rate of $dP/dt = -4.95 \times 10^{-7}$ d yr^{-1}. The photometric solutions are fairly well fitted at a mass ratio of $q = 0.1879$, with a fillout factor of $f = 17.74\%$. The results indicate that there exists mass transfer from the more massive component to the less massive one at a rate of relative mass exchange, $\dot{m}_1/m = -1.09 \times 10^{-7}$ yr^{-1}. It is possible that this weak-contact system, that shows a decreasing orbital period, may undergo contraction of the inner and outer critical Roche lobes and evolve into a deep-contact binary.

Key words: stars: binaries: close — stars: binaries: eclipsing — stars: individual (GV Leo)

1 INTRODUCTION

EW-type binaries have been widely investigated over the past several decades by using both photometric and spectroscopic methods. It is well known that these binaries are classified into two subtypes (Binnendijk 1970). If the more massive component is eclipsed by the less massive one at primary minima, the system is called A-type. On the other hand, a system with the opposite feature is called W-type. Some authors suggested that W-type systems have evolved from A-type ones by mass loss (e.g. Gazeas & Niarchos 2006; Rucinski 1985), whereas others disagreed (e.g. Maceroni et al. 1985; Hilditch et al. 1988). However, van Hamme (1982) and Li et al. (2008) argued that there is no difference between the evolutionary behaviors of both types.

These systems are believed to be formed from detached binaries, which are losing angular momentum and decreasing orbital period by a process called angular momentum loss (AML) (e.g. Vilhu 1981; Rucinski 1982; Li et al. 2004). Under a simplifying assumption that the mass and angular momentum are conserved, contact binaries evolve in a process of mass exchange between both components, which changes their orbital periods and affects their inner and outer critical Roche lobes. Another theory, known as thermal relaxation oscillation (TRO), predicts that the binaries could evolve in a cycle around the marginal contact state, oscillating between contact and semi-detached configurations, depending on the thermal time scale (e.g. Lucy 1976; Robertson & Eggleton 1977). Qian (2001, 2003) proposed that the combination of the TRO and the variable AML can explain the relation between variation of the orbital period and mass ratio for W-type contact binaries, in the

sense that the period change is controlled by the mass ratio. These indicate that the change in orbital period acts as a crucial tracer of the evolution of contact binary systems.

Hut (1980) suggested that if the total spin angular momentum is less than one-third of the orbital angular momentum, these systems are still stable. However, the dynamical evolution could induce contact binaries to evolve into systems with a lower mass ratio and tidal instability forces these systems to merge into rapidly rotating single stars (Li et al. 2008). Furthermore, Rasio & Shapiro (1995) indicated that the decrease in orbital period of a contact binary, controlled by the AML, could pull both components sufficiently close together, bringing the system into a dynamically unstable state, and then forming a single rapidly rotating star.

A contact binary system, GV Leo (RA(2000) = $10^h11^m59.17^s$, Dec.(2000) = $16°52'\,30.1''$) was first identified as an EW-type by Bernhard (2004). Samec et al. (2006) reported that this system showed an orbital period of 0.266758 d, with a mass ratio of 0.1896 and a weak-contact configuration (a Roche lobe fillout of 23%). The O'Connell effect was evident, which indicates magnetic spot activity occurred.

In this study, new CCD photometric data of GV Leo were used to investigate the change in orbital period, derive photometric solutions and investigate the rate of mass transfer between the components. Observations are explained in Section 2. Calculations of the orbital period and the change in period are described in Section 3. Section 4 describes the photometric solutions. Finally, Section 5 contains discussion and conclusions.

2 OBSERVATIONS

Imaging data of GV Leo were obtained from the 0.5-m telescope at Sirindhorn Observatory, Chiang Mai University. The observations were done using an SBIG CCD (Model of ST10-XME), with exposure time of 90 seconds. The photometric data of GV Leo were taken during four nights (2011 February 4–7) using the *BVR* filter bands. We have obtained 248 observations per filter band for GV Leo. The photometric software package IRAF was used to reduce the observed data and measure differential magnitudes in the *BVR* bands.

The differential magnitudes of GV Leo were determined using GSC 1419-1147 (RA(2000) = 10^h11^m 29.85^s, Dec.(2000) = $16°57'51.4''$) and GSC 1419-0805 (RA(2000) = $10^h11^m51.30^s$, Dec.(2000) = $16°50'12.9''$) as comparison and check stars, respectively. The photometric data are listed in Table 1. The amplitudes of light curve variations are approximately 0.43, 0.41 and 0.39 mag, for the *B*-, *V*- and *R*-bands, in that order. There is a magnitude difference between the two maxima. The O'Connell effect is found to be a positive type, i.e., Max.I at phase 0.25 is slightly brighter than Max.II at phase 0.75, with a comparable level of light at the two minima. This is in contrast to what Samec et al. (2006) reported as the opposite type.

3 CHANGE IN ORBITAL PERIOD

New CCD photometric data of GV Leo showed eight times of light minimum in the *BVR* filter bands. Four primary and four secondary minima were found and determined using a least-squares method for each filter band. The times of light minimum in this study were combined with those from literature, to estimate the orbital period, as shown in Table 2. The HJD at light minimum times were fitted with a linear least-squares method and the result yielded the orbital period of 0.26673171($\pm$0.00000013) d as shown in Equation (1).

$$\text{Min.I} = \text{HJD}2455597.2891(\pm0.0007) + 0.26673171(\pm0.00000013) \times E. \qquad (1)$$

The $(O - C)$ values of those eclipse times were determined as listed in Table 2 and the least-squares fitting solution yields Equation (2). The coefficient of the quadratic term indicates that the orbital period decreases at a rate of $dP/dt = -4.95 \times 10^{-7}$ d yr^{-1}.

$$(O - C) = -0.0012(\pm0.0004) - 1.80(\pm0.29) \times 10^{-6}E - 1.81(\pm0.28) \times 10^{-10}E^2. \qquad (2)$$

Table 1 New CCD Photometric Observations in the *BVR* Bands for GV Leo

HJD 2455590+	Δm_B	HJD 2455590+	Δm_V	HJD 2455590+	Δm_R	HJD 2455590+	Δm_B	HJD 2455590+	Δm_V	HJD 2455590+	Δm_R
7.2152	−0.162	7.2141	−0.223	7.2130	−0.299	8.2046	0.151	8.2035	0.055	8.2023	−0.065
7.2194	−0.178	7.2183	−0.238	7.2171	−0.312	8.2085	0.198	8.2074	0.108	8.2063	−0.011
7.2231	−0.175	7.2220	−0.238	7.2209	−0.308	8.2120	0.232	8.2108	0.137	8.2097	0.027
7.2265	−0.172	7.2254	−0.237	7.2243	−0.314	8.2154	0.242	8.2142	0.158	8.2131	0.056
7.2299	−0.158	7.2288	−0.220	7.2277	−0.298	8.2196	0.236	8.2185	0.161	8.2173	0.067
7.2350	−0.138	7.2339	−0.206	7.2327	−0.281	8.2256	0.232	8.2244	0.152	8.2233	0.064
7.2384	−0.129	7.2373	−0.188	7.2362	−0.275	8.2290	0.222	8.2278	0.145	8.2267	0.053
7.2418	−0.117	7.2407	−0.184	7.2396	−0.253	8.2324	0.196	8.2313	0.125	8.2302	0.042
7.2453	−0.100	7.2441	−0.155	7.2430	−0.242	8.2418	0.079	8.2407	0.022	8.2396	−0.049
7.2487	−0.080	7.2476	−0.147	7.2464	−0.232	8.2452	0.033	8.2441	−0.021	8.2430	−0.098
7.2537	−0.038	7.2526	−0.108	7.2515	−0.195	8.2487	0.006	8.2475	−0.049	8.2464	−0.135
7.2575	−0.007	7.2564	−0.085	7.2553	−0.182	8.2527	−0.057	8.2516	−0.095	8.2505	−0.170
7.2657	0.059	7.2646	−0.013	7.2634	−0.109	8.2561	−0.088	8.2550	−0.120	8.2539	−0.198
7.2691	0.103	7.2680	0.027	7.2669	−0.080	8.2596	−0.092	8.2584	−0.150	8.2573	−0.231
7.2725	0.145	7.2714	0.056	7.2703	−0.041	8.2632	−0.121	8.2621	−0.169	8.2610	−0.247
7.2762	0.178	7.2751	0.080	7.2740	−0.015	8.2667	−0.132	8.2655	−0.191	8.2644	−0.267
7.2797	0.210	7.2785	0.123	7.2774	0.026	8.2703	−0.137	8.2692	−0.198	8.2681	−0.274
7.2831	0.232	7.2820	0.150	7.2808	0.052	8.2738	−0.157	8.2726	−0.212	8.2715	−0.285
7.2957	0.236	7.2946	0.162	7.2935	0.069	8.2772	−0.170	8.2760	−0.232	8.2749	−0.298
7.2992	0.210	7.2980	0.136	7.2969	0.056	8.2808	−0.169	8.2796	−0.227	8.2785	−0.299
7.3026	0.175	7.3015	0.115	7.3003	0.035	8.2842	−0.168	8.2830	−0.237	8.2819	−0.301
7.3076	0.105	7.3064	0.057	7.3053	−0.018	8.2921	−0.165	8.2909	−0.235	8.2898	−0.308
7.3144	0.011	7.3133	−0.031	7.3121	−0.100	8.2955	−0.155	8.2944	−0.226	8.2932	−0.311
7.3181	−0.037	7.3170	−0.095	7.3159	−0.143	8.2989	−0.151	8.2978	−0.221	8.2967	−0.306
7.3313	−0.126	7.3302	−0.184	7.3291	−0.247	8.3031	−0.127	8.3020	−0.200	8.3009	−0.287
7.3347	−0.143	7.3336	−0.206	7.3325	−0.259	8.3065	−0.128	8.3054	−0.190	8.3043	−0.265
7.3382	−0.159	7.3370	−0.219	7.3359	−0.283	8.3100	−0.104	8.3088	−0.180	8.3077	−0.257
7.3425	−0.167	7.3414	−0.241	7.3402	−0.302	8.3137	−0.081	8.3126	−0.154	8.3115	−0.247
7.3459	−0.179	7.3448	−0.243	7.3437	−0.313	8.3172	−0.073	8.3160	−0.137	8.3149	−0.225
7.3494	−0.185	7.3482	−0.252	7.3471	−0.316	8.3206	−0.045	8.3195	−0.111	8.3183	−0.202
7.3532	−0.182	7.3521	−0.243	7.3510	−0.319	8.3246	−0.002	8.3234	−0.082	8.3223	−0.175
7.3566	−0.185	7.3555	−0.240	7.3544	−0.329	8.3298	0.054	8.3287	−0.042	8.3276	−0.131
7.3601	−0.177	7.3589	−0.247	7.3578	−0.325	8.3332	0.084	8.3321	0.002	8.3310	−0.095
7.3640	−0.172	7.3629	−0.245	7.3617	−0.326	8.3366	0.123	8.3355	0.035	8.3344	−0.057
7.3708	−0.152	7.3697	−0.222	7.3686	−0.306	8.3413	0.175	8.3402	0.080	8.3391	−0.012
7.3756	−0.141	7.3745	−0.202	7.3734	−0.301	8.3448	0.215	8.3436	0.128	8.3425	0.015
7.3791	−0.129	7.3779	−0.199	7.3768	−0.278	8.3482	0.223	8.3471	0.148	8.3459	0.045
7.3824	−0.109	7.3813	−0.179	7.3802	−0.274	8.3538	0.242	8.3527	0.158	8.3515	0.070
7.3868	−0.083	7.3856	−0.148	7.3845	−0.256	8.3572	0.246	8.3561	0.164	8.3549	0.068
7.3902	−0.040	7.3890	−0.123	7.3879	−0.225	8.3606	0.234	8.3595	0.166	8.3584	0.071
7.3936	−0.010	7.3925	−0.097	7.3913	−0.202	8.3649	0.207	8.3638	0.150	8.3626	0.064
7.3976	0.037	7.3964	−0.055	7.3953	−0.171	8.3683	0.186	8.3672	0.125	8.3661	0.045
7.4010	0.097	7.3999	−0.009	7.3987	−0.134	8.3718	0.131	8.3706	0.079	8.3695	0.015
7.4044	0.121	7.4033	0.044	7.4022	−0.069	8.3759	0.081	8.3747	0.037	8.3736	−0.036
7.4081	0.170	7.4070	0.088	7.4059	−0.030	8.3793	0.034	8.3781	−0.006	8.3770	−0.083
7.4115	0.223	7.4104	0.121	7.4093	0.016	8.3827	−0.014	8.3816	−0.067	8.3804	−0.130
7.4150	0.237	7.4138	0.148	7.4127	0.042	8.3875	−0.058	8.3864	−0.114	8.3852	−0.176
7.4192	0.236	7.4180	0.151	7.4169	0.058	8.3909	−0.077	8.3898	−0.143	8.3887	−0.204
7.4226	0.239	7.4215	0.156	7.4203	0.069	8.3943	−0.098	8.3932	−0.164	8.3921	−0.225
7.4260	0.235	7.4249	0.152	7.4237	0.063	8.3986	−0.132	8.3975	−0.187	8.3964	−0.253
7.4304	0.220	7.4292	0.138	7.4281	0.057	8.4021	−0.148	8.4009	−0.206	8.3998	−0.269
7.4338	0.195	7.4327	0.122	7.4315	0.035	8.4055	−0.164	8.4044	−0.227	8.4032	−0.291
7.4372	0.140	7.4361	0.081	7.4350	−0.008	8.4093	−0.176	8.4082	−0.230	8.4071	−0.300
7.4446	0.057	7.4435	0.000	7.4423	−0.094	8.4127	−0.177	8.4116	−0.245	8.4105	−0.319
7.4480	0.009	7.4469	−0.045	7.4457	−0.125	8.4162	−0.193	8.4150	−0.245	8.4139	−0.322
7.4519	−0.040	7.4508	−0.088	7.4497	−0.161	8.4201	−0.197	8.4190	−0.254	8.4179	−0.321
7.4557	−0.072	7.4546	−0.110	7.4534	−0.195	8.4235	−0.197	8.4224	−0.254	8.4213	−0.324
8.1977	0.041	8.1966	−0.052	8.1955	−0.163	8.4270	−0.189	8.4258	−0.243	8.4247	−0.326
8.2012	0.092	8.2000	0.005	8.1989	−0.109	8.4309	−0.182	8.4298	−0.247	8.4286	−0.318

Table 1 — *Continued.*

HJD 2455590+	Δm_B	HJD 2455590+	Δm_V	HJD 2455590+	Δm_R	HJD 2455590+	Δm_B	HJD 2455590+	Δm_V	HJD 2455590+	Δm_R
8.4343	− 0.173	8.4332	− 0.230	8.4320	− 0.317	9.4217	0.240	9.4205	0.158	9.4194	0.061
8.4377	− 0.164	8.4366	− 0.228	8.4355	− 0.307	9.4251	0.248	9.4240	0.167	9.4228	0.072
9.1917	− 0.090	9.1906	− 0.151	9.1895	− 0.212	9.4285	0.236	9.4274	0.159	9.4262	0.069
9.1952	− 0.106	9.1940	− 0.166	9.1929	− 0.239	9.4319	0.223	9.4308	0.145	9.4296	0.061
9.1986	− 0.125	9.1975	− 0.185	9.1963	− 0.245	9.4353	0.193	9.4342	0.123	9.4330	0.042
9.2050	− 0.161	9.2038	− 0.213	9.2027	− 0.277	9.4387	0.154	9.4376	0.088	9.4364	0.012
9.2084	− 0.169	9.2072	− 0.222	9.2061	− 0.286	10.2086	0.183	10.2074	0.095	10.2063	− 0.013
9.2118	− 0.176	9.2107	− 0.238	9.2095	− 0.308	10.2120	0.210	10.2109	0.135	10.2097	0.029
9.2160	− 0.181	9.2149	− 0.251	9.2138	− 0.313	10.2154	0.239	10.2143	0.159	10.2132	0.055
9.2194	− 0.191	9.2183	− 0.240	9.2172	− 0.327	10.2190	0.248	10.2179	0.167	10.2168	0.070
9.2229	− 0.193	9.2217	− 0.250	9.2206	− 0.323	10.2225	0.247	10.2213	0.160	10.2202	0.062
9.2267	− 0.192	9.2256	− 0.252	9.2245	− 0.322	10.2259	0.235	10.2247	0.154	10.2236	0.063
9.2302	− 0.185	9.2290	− 0.246	9.2279	− 0.324	10.2300	0.210	10.2289	0.139	10.2278	0.055
9.2336	− 0.177	9.2325	− 0.242	9.2313	− 0.320	10.2335	0.180	10.2323	0.120	10.2312	0.037
9.2375	− 0.173	9.2364	− 0.228	9.2352	− 0.310	10.2369	0.150	10.2357	0.090	10.2346	0.011
9.2409	− 0.155	9.2398	− 0.212	9.2386	− 0.306	10.2403	0.108	10.2392	0.055	10.2380	− 0.027
9.2443	− 0.133	9.2432	− 0.198	9.2421	− 0.282	10.2437	0.060	10.2426	0.010	10.2414	− 0.072
9.2486	− 0.111	9.2475	− 0.183	9.2464	− 0.270	10.2478	0.006	10.2467	− 0.042	10.2455	− 0.105
9.2528	− 0.088	9.2516	− 0.160	9.2505	− 0.251	10.2512	− 0.030	10.2501	− 0.089	10.2490	− 0.143
9.2571	− 0.055	9.2560	− 0.127	9.2548	− 0.230	10.2546	− 0.065	10.2535	− 0.122	10.2524	− 0.177
9.2605	− 0.017	9.2594	− 0.085	9.2582	− 0.213	10.2581	− 0.083	10.2569	− 0.148	10.2558	− 0.202
9.2639	0.020	9.2628	− 0.062	9.2617	− 0.173	10.2615	− 0.102	10.2604	− 0.165	10.2592	− 0.232
9.2677	0.079	9.2666	− 0.007	9.2654	− 0.125	10.2655	− 0.125	10.2644	− 0.184	10.2632	− 0.251
9.2711	0.122	9.2700	0.031	9.2689	− 0.079	10.2689	− 0.146	10.2678	− 0.206	10.2667	− 0.261
9.2745	0.163	9.2734	0.078	9.2723	− 0.033	10.2723	− 0.157	10.2712	− 0.225	10.2701	− 0.280
9.2858	0.246	9.2846	0.160	9.2835	0.063	10.2789	− 0.176	10.2778	− 0.231	10.2767	− 0.301
9.2892	0.248	9.2880	0.160	9.2869	0.059	10.2826	− 0.174	10.2815	− 0.245	10.2804	− 0.317
9.2926	0.245	9.2915	0.155	9.2903	0.067	10.2861	− 0.185	10.2849	− 0.243	10.2838	− 0.322
9.2962	0.243	9.2950	0.143	9.2939	0.062	10.2895	− 0.184	10.2884	− 0.254	10.2872	− 0.328
9.2996	0.211	9.2985	0.140	9.2973	0.033	10.2935	− 0.185	10.2924	− 0.250	10.2913	− 0.327
9.3030	0.173	9.3019	0.110	9.3007	0.008	10.2970	− 0.183	10.2958	− 0.236	10.2947	− 0.326
9.3068	0.128	9.3057	0.066	9.3045	− 0.033	10.3004	− 0.162	10.2993	− 0.238	10.2981	− 0.324
9.3102	0.069	9.3091	0.022	9.3080	− 0.069	10.3038	− 0.165	10.3027	− 0.224	10.3016	− 0.318
9.3136	0.026	9.3125	− 0.027	9.3114	− 0.114	10.3077	− 0.141	10.3066	− 0.220	10.3055	− 0.298
9.3171	− 0.008	9.3160	− 0.055	9.3149	− 0.141	10.3111	− 0.137	10.3100	− 0.206	10.3089	− 0.294
9.3206	− 0.063	9.3194	− 0.098	9.3183	− 0.175	10.3145	− 0.122	10.3134	− 0.192	10.3123	− 0.283
9.3240	− 0.080	9.3229	− 0.139	9.3217	− 0.222	10.3180	− 0.102	10.3169	− 0.178	10.3157	− 0.265
9.3415	− 0.154	9.3404	− 0.212	9.3393	− 0.290	10.3217	− 0.068	10.3206	− 0.145	10.3195	− 0.242
9.3449	− 0.160	9.3438	− 0.216	9.3427	− 0.293	10.3252	− 0.043	10.3240	− 0.116	10.3229	− 0.221
9.3483	− 0.169	9.3472	− 0.231	9.3461	− 0.305	10.3286	0.001	10.3275	− 0.085	10.3263	− 0.195
9.3519	− 0.172	9.3507	− 0.227	9.3496	− 0.306	10.3320	0.042	10.3309	− 0.046	10.3298	− 0.159
9.3553	− 0.174	9.3541	− 0.223	9.3530	− 0.302	10.3364	0.104	10.3353	0.018	10.3341	− 0.095
9.3587	− 0.173	9.3576	− 0.229	9.3564	− 0.311	10.3398	0.146	10.3387	0.058	10.3376	− 0.063
9.3626	− 0.160	9.3615	− 0.221	9.3604	− 0.299	10.3432	0.203	10.3421	0.112	10.3410	0.005
9.3660	− 0.146	9.3649	− 0.214	9.3638	− 0.292	10.3467	0.240	10.3455	0.144	10.3444	0.035
9.3694	− 0.134	9.3683	− 0.199	9.3672	− 0.290	10.3501	0.236	10.3490	0.146	10.3478	0.060
9.3754	− 0.110	9.3743	− 0.174	9.3731	− 0.259	10.3542	0.246	10.3531	0.157	10.3519	0.055
9.3788	− 0.097	9.3777	− 0.151	9.3766	− 0.247	10.3576	0.241	10.3565	0.152	10.3553	0.064
9.3822	− 0.074	9.3811	− 0.133	9.3800	− 0.241	10.3610	0.233	10.3599	0.161	10.3588	0.061
9.3859	− 0.063	9.3847	− 0.128	9.3836	− 0.206	10.3644	0.235	10.3633	0.152	10.3622	0.047
9.3893	− 0.018	9.3882	− 0.090	9.3871	− 0.192	10.3679	0.187	10.3667	0.130	10.3656	0.026
9.3927	0.001	9.3916	− 0.073	9.3905	− 0.162	10.3716	0.156	10.3705	0.095	10.3693	0.002
9.3964	0.039	9.3952	− 0.048	9.3941	− 0.140	10.3750	0.108	10.3739	0.036	10.3728	− 0.030
9.3998	0.077	9.3987	− 0.010	9.3975	− 0.103	10.3784	0.057	10.3773	0.007	10.3762	− 0.088
9.4032	0.118	9.4021	0.023	9.4010	− 0.064	10.3819	0.015	10.3807	− 0.041	10.3796	− 0.130
9.4078	0.156	9.4067	0.073	9.4056	− 0.033	10.3853	− 0.014	10.3842	− 0.086	10.3830	− 0.159
9.4113	0.201	9.4101	0.090	9.4090	0.018	10.3962	− 0.101	10.3951	− 0.162	10.3939	− 0.241
9.4147	0.222	9.4135	0.145	9.4124	0.039	10.4003	− 0.126	10.3992	− 0.186	10.3980	− 0.257
9.4182	0.242	9.4171	0.155	9.4160	0.062	10.4037	− 0.144	10.4026	− 0.198	10.4015	− 0.273

Table 1 — *Continued.*

HJD 2455590+	Δm_B	HJD 2455590+	Δm_V	HJD 2455590+	Δm_R	HJD 2455590+	Δm_B	HJD 2455590+	Δm_V	HJD 2455590+	Δm_R
10.4071	-0.144	10.4060	-0.213	10.4049	-0.280	10.4291	-0.164	10.4280	-0.227	10.4269	-0.306
10.4106	-0.162	10.4094	-0.221	10.4083	-0.295	10.4325	-0.146	10.4314	-0.216	10.4303	-0.300
10.4140	-0.174	10.4128	-0.227	10.4117	-0.305	10.4360	-0.141	10.4348	-0.212	10.4337	-0.298
10.4181	-0.162	10.4169	-0.233	10.4158	-0.305	10.4398	-0.132	10.4398	-0.198	10.4375	-0.277
10.4215	-0.169	10.4204	-0.231	10.4192	-0.309	10.4432	-0.108	10.4432	-0.171	10.4410	-0.262
10.4249	-0.168	10.4238	-0.228	10.4227	-0.314	10.4466	-0.085	10.4466	-0.151	10.4444	-0.241

Table 2 All Times of Light Minimum for GV Leo

HJD (1)	Epoch (2)	Min (3)	$(O-C)$ (4)	Ref. (5)
2452754.4598	-10658.0	I	-0.0027	[1]
2452763.3966	-10624.5	II	-0.0015	[2]
2452764.4639	-10620.5	II	-0.0011	[2]
2453437.6973	-8096.5	II	0.0015	[3]
2453437.8293	-8096.0	I	0.0001	[3]
2453441.8291	-8081.0	I	-0.0011	[3]
2454506.4949	-4089.5	II	0.0051	[4]
2454507.5613	-4085.5	II	0.0046	[5]
2454908.4567	-2582.5	II	0.0022	[6]
2454935.3964	-2481.5	II	0.0020	[6]
2455289.3487	-1154.5	II	0.0013	[7]
2455289.4810	-1154.0	I	0.0003	[7]
2455597.2876	0.0	I	-0.0015	[*]
2455597.4217	0.5	II	-0.0008	[*]
2455598.2199	3.5	II	-0.0028	[*]
2455598.3543	4.0	I	-0.0018	[*]
2455599.2890	7.5	II	-0.0006	[*]
2455599.4238	8.0	I	0.0008	[*]
2455600.2203	11.0	I	-0.0029	[*]
2455600.3555	11.5	II	-0.0011	[*]

Notes: Col. (1): HJD at light minimum. Col. (2): epoch. Col. (3): types of minimum. Col. (4): residuals of HJD at light minimum. Col. (5): references for sources are as follows, [1] Hübscher (2005); [2] Bernhard (2004); [3] Samec et al. (2006); [4] Hübscher et al. (2010); [5] Brát et al. (2008); [6] Brát et al. (2009); [7] Hübscher & Monninger (2011); [*] This study.

The corresponding $(O-C)$ curve is shown as a downward parabolic line in the upper panel and the residuals are shown in the lower panel of Figure 1.

4 PHOTOMETRIC SOLUTIONS

Photometric solutions of GV Leo were deduced by using the 2003 version of the Wilson-Devinney (W-D) code (Wilson & Devinney 1971; Wilson 1979, 1990; Wilson & van Hamme 2003), in mode 3 (i.e., contact mode). Fixed parameters were adopted as follows: the gravity darkening exponents of $g_1 = g_2 = 0.32$ (Lucy 1967), the bolometric albedo coefficients of $A_1 = A_2 = 0.50$ (Rucinski 1973), the effective temperature of the primary component, T_1, was estimated from $(B-V)$ color by using Cox (2000)'s calibration table, and then the temperature T_1 was used to calculate the corresponding limb darkening coefficients of x_1 and x_2 for the *BVR* bands (van Hamme 1993). The adjustable parameters, i.e., the orbital inclination, i, estimated temperature of the secondary component, T_2,

**Table 3** Photometric Solutions for the Light Curve Fits of GV Leo

Parameter	Value
q	0.1879 ($\pm$0.0024)
T_1 (K)	4850
T_2 (K)	5344 ($\pm$26)
i (°)	76.13 ($\pm$0.32)
$\Omega_1 = \Omega_2$	2.181 ($\pm$0.0051)
$g_1 = g_2$	0.32
$A_1 = A_2$	0.50
$x_{1B} = x_{2B}$	0.891
$x_{1V} = x_{2V}$	0.729
$x_{1R} = x_{2R}$	0.571
$L_{1B}/(L_{1B} + L_{2B})$	0.6988 ($\pm$0.0051)
$L_{1V}/(L_{1V} + L_{2V})$	0.7241 ($\pm$0.0036)
$L_{1R}/(L_{1R} + L_{2R})$	0.7467 ($\pm$0.0027)
$L_{3B}/(L_{1B} + L_{2B} + L_{3B})$	0.0114 ($\pm$0.0010)
$L_{3V}/(L_{1V} + L_{2V} + L_{3V})$	0.0169 ($\pm$0.0010)
$L_{3R}/(L_{1R} + L_{2R} + L_{3R})$	0.0247 ($\pm$0.0011)
r_1 (pole)	0.4968 ($\pm$0.0013)
r_1 (side)	0.5433 ($\pm$0.0020)
r_1 (back)	0.5670 ($\pm$0.0026)
r_2 (pole)	0.2345 ($\pm$0.0037)
r_2 (side)	0.2446 ($\pm$0.0045)
r_2 (back)	0.2824 ($\pm$0.0092)
Spot Colatitude (°) *	37.24 ($\pm$3.96)
Spot Longitude (°) *	14.32 ($\pm$2.78)
Spot Radius (°) *	25.79 ($\pm$1.37)
Temperature Factor *	0.80 ($\pm$0.02)
$\Sigma(O - C)^2$	0.0635
f (%)	17.7 4($\pm$3.66)

Notes: * Parameters of a starspot on the primary component.

the mass ratio, q, the surface potential of the components, $\Omega_1 = \Omega_2$, and the monochromatic luminosities of the star 1, L_1, were adopted to deduce the photometric solutions. The relative luminosities of star 2, L_2, were automatically determined by the W-D code, following the model of stellar atmospheres (Kurucz 1993).

Due to the $(B - V)$ color of the comparison star, GSC 1419–1147 is a very stable, normal star; the value $(B - V)_{\text{comparison}} = 0.977$ was collected from the Tycho-2 Catalogue (Høg et al. 2000). However, our data gave $(B - V)_{\text{GV Leo}} - (B - V)_{\text{comparison}} = 0.07$. With correction of $(B - V)_{\text{Johnson}} = 0.85\,(B - V)_{\text{Tycho}}$ (Gürol et al. 2011), the calculated $(B - V)$ color of GV Leo was found to be $(B - V)_{\text{GV Leo}} = 0.90$. Thus, the effective temperature of the primary component, T_1, was assumed to be 4850 K (Cox 2000). As a result, the limb darkening coefficients were fixed at $x_{1B} = x_{2B} = 0.891$, $x_{1V} = x_{2V} = 0.729$ and $x_{1R} = x_{2R} = 0.571$ (van Hamme 1993).

The observed light curves in the *BVR* filter bands of GV Leo agree with the photometric parameters, as listed in Table 3. The photometric solutions show that this system is an A-type contact binary. The derived mass ratio, q, is 0.1879 ($\pm$0.0024), with the sum of squared residuals for input values, $\Sigma(O - C)^2 = 0.0635$, corresponding the theoretical light curves, which are plotted in Figure 2. The asymmetric light curves can be explained by the activity of a cool spot on the primary component. The geometric contact degree, f, is found to be 17.74% ($\pm$3.66%), which is not very different from what Samec et al. (2006) found. This indicates that GV Leo is still in a weak-contact state.
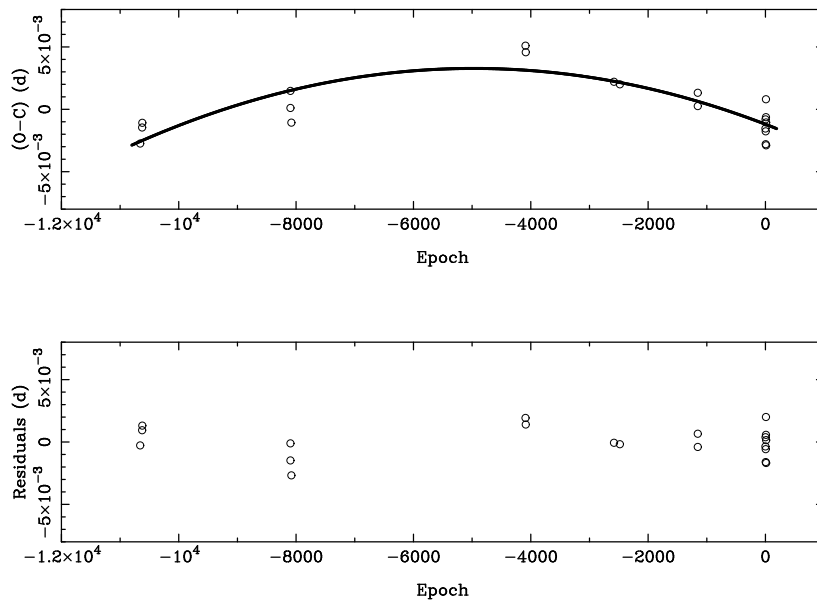
Fig. 1 ($O - C$) curve (*upper panel*) and the corresponding residuals (*lower panel*) for GV Leo.
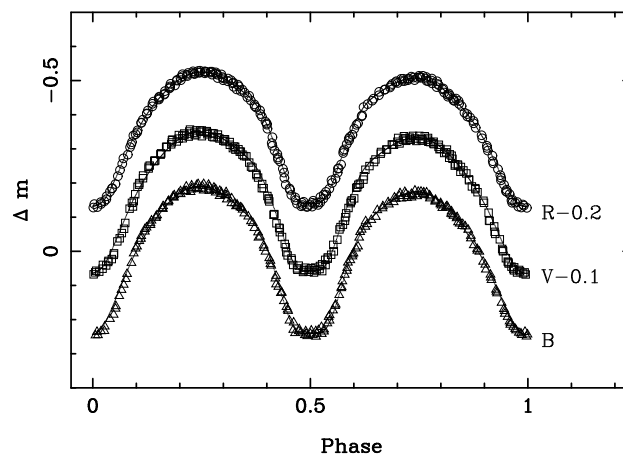
Fig. 2 Observed differential magnitudes in the B (*triangle*), V (*square*) and R (*circle*) filter bands and their theoretical light curves (*solid lines*) versus orbital phase for GV Leo.

5 DISCUSSION AND CONCLUSIONS

The change in orbital period of GV Leo is consistent with what systems with a low mass ratio usually show in terms of period decrease as suggested by Qian (2001). The orbital period of this low-mass ratio contact binary is decreasing at a rate of $dP/dt = -4.95 \times 10^{-7}$ d yr^{-1}. One possibility is that the orbital period could be changed by a process of mass transfer between both components. Under the assumption of conservative mass transfer, without mass loss or variation in the angular momentum,

the relative mass transfer rate, $\dot{m}_1/m$, can be estimated by using the following equation (Singh & Chaubey 1986; Pribulla 1998)

$$\frac{\dot{P}}{P} = \frac{3(1-q^2)}{q}\frac{\dot{m}_1}{m}, \tag{3}$$

where $\dot{m}_1$ is mass increase of the more massive component ($\dot{m}_1 = -\dot{m}_2$), m is total mass ($m = m_1 + m_2$), and q is the mass ratio of the less to more massive components. As a result, the process of mass transfer from the more massive component to the less massive one is occurring, with the rate of relative mass transfer being $\dot{m}_1/m = -1.09\times10^{-7}$ yr^{-1}.

GV Leo is a shallow contact binary with a decreasing orbital period, like BI CVn (Qian et al. 2008), WZ Cep (Zhu & Qian 2009), AH Tau (Yang et al. 2010) and BS Cas (He et al. 2010). With the decrease of the orbital period, the system may undergo a state of AML via magnetic stellar wind (Rasio & Shapiro 1995; Qian 2001). The inner and outer critical Roche lobes will contract and cause the degree of contact to increase. Thus, GV Leo may evolve into a deeper contact configuration, similar to IK Per (Zhu et al. 2005), GR Vir (Qian & Yang 2004), and FG Hya (Qian & Yang 2005). However, further photometric and spectroscopic observations are still required to investigate the long-term change in period and other physical properties.

References

Bernhard, K. 2004, Berliner Arbeitsgemeinschaft fuer Veraenderliche Sterne - Mitteilungen, 168, 1

Binnendijk, L. 1970, Vistas in Astronomy, 12, 217

Brát, L., Šmelcer, L., Kuèáková, H., et al. 2008, Open European Journal on Variable Stars, 94, 1

Brat, L., Trnka, J., Lehky, M., et al. 2009, Open European Journal on Variable Stars, 107, 1

Cox, A. N. (ed.) 2000, Allen's Astrophysical Quantities (4th ed.; New York: Springer), 388

Gazeas, K. D., & Niarchos, P. G. 2006, MNRAS, 370, L29

Gürol, B., Derman, E., Saguner, T., et al. 2011, New Astron., 16, 242

He, J.-J., Qian, S.-B., Zejda, M., & Mikulášek, Z. 2010, RAA (Research in Astronomy and Astrophysics), 10, 569

Hilditch, R. W., King, D. J., & McFarlane, T. M. 1988, MNRAS, 231, 341

Høg, E., Fabricius, C., Makarov, V. V., et al. 2000, A&A, 355, L27

Hubscher, J. 2005, Information Bulletin on Variable Stars, 5643, 1

Hubscher, J., Lehmann, P. B., Monninger, G., Steinbach, H.-M., & Walter, F. 2010, Information Bulletin on Variable Stars, 5918, 1

Hubscher, J., & Monninger, G. 2011, Information Bulletin on Variable Stars, 5959, 1

Hut, P. 1980, A&A, 92, 167

Kurucz, R. L. 1993, in Light Curve Modeling of Eclipsing Binary Stars, ed. E. F. Milone (New York: Springer-Verlag), 93

Li, L., Han, Z., & Zhang, F. 2004, MNRAS, 355, 1383

Li, L., Zhang, F., Han, Z., Jiang, D., & Jiang, T. 2008, MNRAS, 387, 97

Lucy, L. B. 1967, ZAp, 65, 89

Lucy, L. B. 1976, ApJ, 205, 208

Maceroni, C., Milano, L., & Russo, G. 1985, MNRAS, 217, 843

Pribulla, T. 1998, Contributions of the Astronomical Observatory Skalnate Pleso, 28, 101

Qian, S. 2001, MNRAS, 328, 635

Qian, S. 2003, MNRAS, 342, 1260

Qian, S.-B., & Yang, Y.-G. 2004, AJ, 128, 2430

Qian, S., & Yang, Y. 2005, MNRAS, 356, 765

Qian, S.-B., He, J.-J., Liu, L., Zhu, L.-Y., & Liao, W. P. 2008, AJ, 136, 2493

Rasio, F. A., & Shapiro, S. L. 1995, ApJ, 438, 887

Robertson, J. A., & Eggleton, P. P. 1977, MNRAS, 179, 359

Ruciński, S. M. 1973, Acta Astronomica, 23, 79

Rucinski, S. M. 1982, A&A, 112, 273

Rucinski, S. M. 1985, in NATO ASIC Proc. 150: Interacting Binaries, eds. P. P. Eggleton & J. E. Pringle, 13

Samec, R. G., Scott, T. D., Branning, J. S., et al. 2006, Information Bulletin on Variable Stars, 5697, 1

Singh, M., & Chaubey, U. S. 1986, Ap&SS, 124, 389

van Hamme, W. 1982, A&A, 105, 389

van Hamme, W. 1993, AJ, 106, 2096

Vilhu, O. 1981, Ap&SS, 78, 401

Wilson, R. E. 1979, ApJ, 234, 1054

Wilson, R. E. 1990, ApJ, 356, 613

Wilson, R. E., & Devinney, E. J. 1971, ApJ, 166, 605

Wilson, R. E., & Van Hamme, W. 2003, Computing Binary Stars Observables (the 4th edition of the W-D Program)

Yang, Y.-G., Wei, J.-Y., Kreiner, J. M., & Li, H.-L. 2010, AJ, 139, 195

Zhu, L. Y., & Qian, S. B. 2009, AJ, 138, 2002

Zhu, L.-Y., Qian, S.-B., Soonthornthum, B., & Yang, Y.-G. 2005, AJ, 129, 2806